Proc. of the Intl. Conf. on Advances in Structural,Civil and Environmental Engineering -- SCEE 2013

ISBN: 978-981-07-6261-2

Dynamic response of axially loaded Timoshenko beams with intermediate fixities to repeated transient hydrodynamic impact loads

Nabanita Datta
Dept. Of Ocean Engg. & Naval Architecture
IIT Kharagpur
Kharagpur,India

Mohd Atif Siddiqui
Dept. Of Ocean Engg. & Naval Architecture
IIT Kharagpur
Kharagpur,India

Abstract

A dynamic analysis of axially loaded Timoshenko beams with intermediate fixities is presented. The underwater part of a craft is modeled as a flexible beam, which rises out and slams against the water at a large vertical velocity, causing highly localized hydrodynamic impact pressure moving at high velocities across the beam, setting it into high-frequency vibrations. The beam natural frequencies depend on the slenderness ratio, axial load, and end fixities. Increasing the axial tension and/or end fixity increases the natural frequencies, which are generated through Eigen analysis.

Next, normal mode summation is used to analyze the impact-induced vibration response, which is generated for various impact speeds, deadrise angles, end fixities, axial loads, and slenderness ratios of the beam. A parametric study is done to predict the maximum dynamic stresses on the structure. The pressure is assumed to act at the equilibrium position. The aim is to study the dynamic stress configurations and draw conclusions leading to sound structural designs.

Keywords **Slamming, Impact loads, Beam vibration, Dynamic stresses, Normal mode analysis.**

1. Introduction

As conventional ship design gives way to non-conventional high performance marine vehicles, structural analysis of high speed crafts becomes the cornerstone of a sound structural design. Crafts like planning crafts, hydrofoil crafts, catamarans, surface-effect ships (SES) are subject to various dynamic loads during their operation. Dynamic lift due to planing leads to emergence of the craft above its zero-speed waterline. This changed attitude greatly changes the seakeeping and dynamic effects of the craft (slamming, deck-wetness, sea-sickness, etc). Changing forward speeds of the craft and sea states change the dynamic lift produced, leading to a certain probability of slam, which is the product of the probability of forefoot emergence and the probability of exceedance of the vertical velocity over a threshold velocity.

Bokaian (1990) studied the free vibration of axially loaded Timoshenko beams, with classical end conditions. Lin (1994) studied the vibration of simply-supported Timoshenko beams to moving point loads, using Finite Element Analysis. This study was limited to a point load, and a single boundary condition of the beam. Axial tension was also absent. Chang (1994) studied Timoshenko beams on elastic foundations and axial loads, but the external force was limited to point loads, varying randomly in time. The end conditions of the beam remained simply-supported. Farchaly and Shebl (1995) studied the frequencies and modeshapes of Timoshenko beams with intermediate fixities and elastic end supports. This study was limited to free vibration only. Wang (1997) studied the vibration of multi-span Timoshenko beams to point moving loads, using the normal mode summation method. The forced vibration was comparatively done for both Euler-Bernoulli and Timoshenko beams. Majkut (2009) solved the vibration of Timoshenko beams by the Green's function method, since the forcing was a Dirac Delta function in space. The natural frequencies and modeshapes of a Timoshenko beam have been compared to those of a Euler-Bernoulli beam, for various classical end conditions.

None of the above has explored the vibratory dynamics of a beam under loads similar to the hydrodynamic impact configurations.

In this work, the underwater part of the craft is modeled as an axially loaded Timoshenko beam, with intermediate end fixities. First, the free vibration analysis has been done by the Eigen Value method, in order to generate the natural frequencies and modeshapes. The

Proc. of the Intl. Conf. on Advances in Structural,Civil and Environmental Engineering -- SCEE 2013

ISBN: 978-981-07-6261-2

free vibration frequencies, with and without axial tension, have been tabulated for various end fixities. The beam is then subjected to two configurations of the stretching hydrodynamic transient load : (a) uniform stretching load of unit magnitude, and (b) Impact load configuration at various deadrise angles. The dynamic analysis has been done by the normal mode summation method, while the static analysis has been done by the Galerkin's method. The maximum dynamic overshoot over the maximum static deflection generates the dynamic loading factor (DLF) for various speeds of the transient load. The wetting time of the plate has been non-dimensionalized by the first natural frequency of the beam, to generate the non-dimensional wetting time τ. The DLF vs. τ characteristics have been generated for the Timoshenko beam with several different end fixities, with and without tension, and some structural damping. The range of τ, for which the beam shows pronounced dynamic behavior has been established. This leads to insights leading to sound structural recommendations.

2. Problem formulation

The underwater part of the vessel (Fig.1) is modeled as a lightly damped Timoshenko beam, at a deadrise angle of β degrees to the horizontal, which impacts against the water surface as a vertical velocity V m/sec; which is the velocity of the relative bow motion, i.e. the net velocity of heave, pitch, and wave elevation at that location, including the phase differences. The beam may be axially loaded either in compression or in tension. The end fixities vary from 0% (Simply-supported beam) to 100% (Clamped-clamped beam), depending on the quality of the welding. The hydrodynamic impact causes a very high magnitude, localized, transient pressure to move across the length of the beam; setting it into high-frequency vibrations, causing bending stress and shear stress waves along the length of the beam. The length varies along x (metres), and the time is denoted as t (seconds). The x=0 and x=L locations typically correspond to the longitudinal stiffeners of the craft. The total out-out-plane transverse flexural deflection of the beam is denoted as z(x,t), varying as a function of space and time. The structural damping is assumed to be zero, since marine structures are usually very lightly damped. The maximum deflection is assumed to occur early in the impact sequence, and hence the analysis is done for dry vibrations, ignoring the fluid inertia (added masses) of the surrounding water. The wetdeck vibrations of a catamaran, after such an impact, are almost always dry vibrations. The high frequency limit of structural oscillations leads to a nearly calm water free-surface condition (rigid lid condition). The radiation damping is considered to be zero.

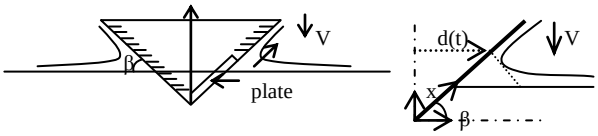

Fig. 1 Cross-sectional slamming model of a typical high-speed craft.

The moving force f(x,t) N/m is modeled as a function of space and time. Two forcing configurations are used as follows :

(1) **Uniform stretching load configuration** (Single sweep).

In this benchmark forcing case, a force of unit magnitude F(x,t) = 1 N/m stretches across the length L of the beam at different speeds c, such that the wetting time is L/c, as shown in Fig.2. This configuration models the progressive wetting of the beam upon entering the water. The wetting time is non-dimensionalized by the first natural period of the beam. The non-D splash time is defined as $\tau = \frac{L}{c}\frac{\omega_{n1}}{2\pi}$. This combines the two time-scales of the problem into one.

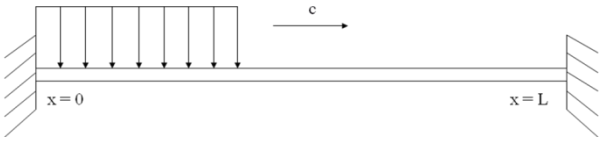

Fig.2 Uniform stretching load of unit magnitude.

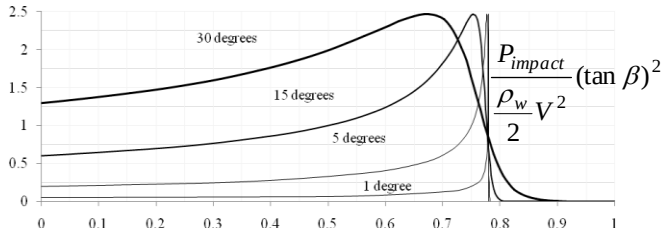

Fig.3 Hydrodynamic impact load (non-D).

(2) **Impact force configuration of the impact force**

As shown in Fig.3, here the sweeping force rises to a peak value and drops to nearly zero. The keel pressure remains the same, while the force stretches across the beam at a speed $\frac{V\pi}{2\sin\beta}$. The wetting speed, the peak pressure, and the loading configuration, depend on the impact velocity V and the deadrise angle β. The smaller the deadrise angle, the greater is the peak pressure, more

Proc. of the Intl. Conf. on Advances in Structural,Civil and Environmental Engineering -- SCEE 2013

ISBN: 978-981-07-6261-2

concentrated is the forcing configuration, and faster is the wetting.

Table 1 : Impact pressure characteristics for V = 10 m/sec

Deadrise angle	$\frac{\dot{d}(t)}{V}$	T_{sp}	$\frac{P_{peak}}{P_{stag}}$	$\frac{P_{keel}}{P_{stag}}$
1 degree	90.00457	0.11	8100.823	180.0091
5 degrees	18.02287	0.56	324.8237	36.04573
15 degrees	6.069091	1.65	36.83387	12.13818
30 degrees	3.141593	3.18	9.869604	6.283185

The jet head is given as $d(t) = \frac{Vt\pi}{2\tan\beta}$, the jet head velocity is $\dot{d}(t) = \frac{V\pi}{2\tan\beta}$. The constant keel pressure is given as $P(0,t) = \rho_{water} V \dot{d}(t)$ and the transient peak pressure is expressed as $P_{peak} = \frac{\rho_{water}}{2}\left[\dot{d}(t)\right]^2$, which are the two constants of the stretching load. The stagnation pressure of the vertical impact velocity is given as $P_{stagnation} = \frac{\rho_{water}}{2} V^2$. Including the rise-up of the water due to the impact, the wetting time is defined and non-dimensionalized by the fundamental natural period of the beam, as:

$$T_{sp} = \frac{2L\sin\beta}{V\pi},\quad \tau = \frac{2L\sin\beta}{V\pi}\frac{\omega_{1,dry}}{2\pi}\sqrt{1-\zeta^2}.$$

Table 1 shows above characteristics of the impact pressure at four different deadrise angles, at V = 10m/sec. The pressure distribution, at any instant, is assumed to be a parabolic distribution, emulating the Wagner's impact pressure model. With x_w as the wetted length as a given instant of time,

$$P(x,t) = P_{keel} + \frac{x^2}{4a},\quad a = \frac{x_w^2}{4(P_{peak} - P_{keel})},\quad x_w = \frac{Vt\pi}{2\sin\beta}.$$

Repeated impacts cause cumulative deflections and stresses in the beam. The subsequent forcing configurations are assumed to act on the deformed beam. The duration between two consecutive slams is calculated through the probability if slamming. Forefoot emergence is the necessary condition for slam, and exceedance of the threshold vertical velocity is the sufficient condition. This threshold velocity differs for different deadrise angles.

3. Analysis methodology

The system of simultaneous governing differential equations of impact-induced undamped free vibration of an axially loaded Timoshenko beam, utilizing Newton's second law, is given as follows :

$$\rho A\frac{\partial^2 z(x,t)}{\partial t^2} = \mu AG\left[\frac{\partial^2 z(x,t)}{\partial x^2} - \frac{\partial\varphi(x,t)}{\partial x}\right] \pm N\frac{\partial^2 z(x,t)}{\partial x^2};$$

$$\rho I\frac{\partial^2\varphi(x,t)}{\partial t^2} = \mu AG\left[\frac{\partial z(x,t)}{\partial x} - \varphi(x,t)\right] + EI\frac{\partial^2\varphi(x,t)}{\partial x^2} \text{ Or}$$

$$\rho A\ddot{z} = \mu AG\left[z'' - \varphi'\right] \pm Nz'';\ \rho I\ddot{\varphi} = \mu AG\left[z' - \varphi\right] + EI\varphi'' \pm Nz'$$

Eq. 1(A,B)

Eq.1(A) is a force balance equation, while Eq.1(B) is a moment balance equation, per unit length. The axial force N is positive for tensile force and negative for compressive force. Here, $z(x,t)$ is the deflection and $\varphi(x,t)$ is the bending slope, as functions of space and time. ρ is the density of the beam, A is the cross-sectional area of the beam, I is the second moment of area of the cross-sectional are of the beam about the horizontal neutral axis, E is the elastic modulus and G is the shear modulus of the material, and μ is the Timoshenko shear coefficient (=5/6 for a rectangular section). The shear deformation and rotary inertia are included in the beam analysis. The shear strain is assumed constant over a given cross-section.

The four boundary conditions are expressed as:

$$z(0,t) = 0;\ z(L,t) = 0;\ EI\frac{\partial^2 z(0,t)}{\partial x^2} = K_{\theta L}\frac{\partial z(0,t)}{\partial x};$$

$$EI\frac{\partial^2 z(L,t)}{\partial x^2} = -K_{\theta R}\frac{\partial z(L,t)}{\partial x}.$$

The displacement is zero at the ends, while the bending moment at the end equals the restraining moment at the ends. The end fixities are modeled as torsional springs at the left and right ends, with torsional spring constants $K_{\theta L}$ and $K_{\theta R}$. As these spring constants tend to zero, the end bending moments vanish and the beam approaches a simply supported beam. As these spring constant tend to infinity, the end slopes vanish and the beam approaches a clamped-clamped beam.

3.1 Free Vibration

The total deflection $z(x,t)$ and bending slope $\varphi(x,t)$ are given as a superposition of the modeshapes (in space) and principal coordinates (in time). Here, $\phi_j(x)$ is the j[th] beam modeshape, and $\psi_j(x)$ is the j[th] bending slope modeshape. The total deflection is a sum of (a) pure bending deflection, which is given by the Euler-Bernoulli beam theory, and (b) the shear deflection. The total slope is a sum of the pure bending slope and the shear deflection slope. They are respectively expressed as

$$z(x,t) = \sum_{j=1}^{\infty}\phi_j(x)\ q_j(t) \text{ and } \varphi(x,t) = \sum_{j=1}^{\infty}\psi_j(x)\ q_j(t).$$

Proc. of the Intl. Conf. on Advances in Structural,Civil and Environmental Engineering -- SCEE 2013

ISBN: 978-981-07-6261-2

Separation of the variables leads to a fourth order equation in space, and a second order equation in time. Euler-Bernoulli beams generate a unique frequency parameter, corresponding to a single natural frequency. The process followed is similar to that given by Chang (1994). Timoshenko beams have a pair of frequency parameters associated with a unique natural frequency. Substitution of the boundary conditions leads to a transcendental equation, solved by the Newton-Raphson method to generate the pairs of frequency-parameters.

3.2 Forced Vibration

The system of simultaneous governing differential equations of impact-induced undamped forced vibration of an axially loaded Timoshenko beam, utilizing Newton's second law, is given by Eq.2(A,B), as follows :

$$\rho A\ddot{z}(x,t) = \mu AG\left[z''(x,t) - \varphi'(x,t)\right] + F(x,t) \pm Nz''(x,t);$$
$$\rho I\ddot{\varphi}(x,t) = \mu AG\left[z'(x,t) - \varphi(x,t)\right] + EI\varphi''(x,t).$$

Eq.2(A,B)

3.2.1 Dynamic Analysis

The shear deformation and rotary inertia are both included in the dynamic analysis. Using the modal expansion for the deflection and the bending slope, the system of equation is expressed as

$$\rho A\sum_{j=1}^{\infty}\phi_j(x)\,\ddot{q}_j(t) = F(x,t) \pm N\sum_{j=1}^{\infty}\phi_j''(x)\,q_j(t) + \mu AG\left[\sum_{j=1}^{\infty}\phi_j''(x)\,q_j(t) - \sum_{j=1}^{\infty}\psi_j'(x)\,q_j(t)\right]$$

$$\rho I\sum_{j=1}^{\infty}\psi_j(x)\,\ddot{q}_j(t) = EI\sum_{j=1}^{\infty}\psi_j''(x)\,q_j(t) + \mu AG\left[\sum_{j=1}^{\infty}\phi_j'(x)\,q_j(t) - \sum_{j=1}^{\infty}\psi_j(x)\,q_j(t)\right].$$

Eq.3(A,B)

Eq.3(A) is pre-multiplied by $\phi_k(x)$ and integrated over the length L, to generate Eq.4(A). Eq.3(B) is pre-multiplied by $\psi_k(x)$ and integrated over the length L, to generate Eq.4(B).

$$\sum_{j=1}^{\infty}GM_{kj}\,\ddot{q}_j(t) = GF_k(t) \pm \sum_{j=1}^{\infty}GN_{kj}\,q_j(t) + \left[\sum_{j=1}^{\infty}GS1_{kj}q_j(t) - \sum_{j=1}^{\infty}GS2_{kj}q_j(t)\right]$$

$$\sum_{j=1}^{\infty}GR_{kj}\,\ddot{q}_j(t) = \sum_{j=1}^{\infty}GK_{kj}\,q_j(t) + \left[\sum_{j=1}^{\infty}GS3_{kj}\,q_j(t) - \sum_{j=1}^{\infty}GS4_{kj}q_j(t)\right].$$

Where

$$GM_{kj} = \rho A\int_L \phi_k\phi_j\,dx,\ GF_k(t) = \int_L \phi_k F\,dx,\ GN_{kj} = N\int_L \phi_k\phi_j''\,dx$$

$$GS1_{kj} = \mu AG\int_L \phi_k\phi_j''\,dx,\ GS2_{kj} = \mu AG\int_L \phi_k\psi_j'\,dx,$$

$$GR_{kj} = \rho I\int_L \psi_k\psi_j\,dx,\ GK_{kj} = EI\int_L \psi_k\psi_j''\,dx,$$

$$GS3_{kj} = \mu AG\int_L \psi_k\phi_j'\,dx,\ GS4_{kj} = \mu AG\int_L \psi_k\psi_j\,dx.$$

The beam modeshapes are orthogonal to each other, and the beam-slope modeshapes are also orthogonal to each other. Writing it in the matrix form, the system of equations becomes :

$$[GM]\{\ddot{q}\} + [GC]\{\dot{q}\} - [GS1]\{q\} + [GS2]\{q\} \pm [GN]\{q\} = \{GF\}$$
$$[GR]\{\ddot{q}\} - [GS3]\{q\} + [GS4]\{q\} - [GK]\{q\} = \{0\}$$

Eq.4(A,B)

Proportional structural damping is included, which manifests in the first equation above as the generalized damping $[GC] = 2\zeta\sqrt{[GK][GM]}$, where ζ is the damping ratio and $2\sqrt{[GK][GM]}$ can be considered to be the modal critical damping. The physical structural damping has not been explicitly defined here. The combined equation is written as :

$$[GM + GR]\{\ddot{q}(t)\} + [GC]\{\dot{q}(t)\} + [GS]\{q(t)\} - [GK]\{q(t)\} \pm [GN]\{q(t)\} = \{GF(t)\},$$

Eq.5

where $[GS] = -[GS1] + [GS2] - [GS3] + [GS4]$.

The advantage of the normal mode summation is that the two coupled governing differential equations can be written as a single equation as a function of time. Eq.5 is solved simultaneously by the Euler-implicit-explicit time-integrator method to generate the principal coordinates as functions of time, which are then pre-multiplied by the beam modes and slope modes to generate the deflection and bending slope respectively, as functions of space and time.

3.2.2 Static Analysis

Only the shear deformation gets included in the static analysis. The system of simultaneous governing differential equations of forced quasi-static deflection of an axially loaded Timoshenko beam, utilizing Newton's second law, is given as follows :

$$\mu AG\left[z''(x,t) - \varphi'(x,t)\right] + F(x,t) \pm Nz''(x,t) = 0;$$
$$\mu AG\left[z'(x,t) - \varphi(x,t)\right] + EI\varphi''(x,t) \pm Nz'(x,t) = 0.$$

Eq.6

Eliminating the pure bending slope $\varphi(x,t)$ from the above system of coupled static equations, we get

Proc. of the Intl. Conf. on Advances in Structural,Civil and Environmental Engineering -- SCEE 2013

ISBN: 978-981-07-6261-2

$$EI\left(1 \pm \frac{N}{\mu AG}\right) z_{st}^{IV}(x,t) \pm N z_{st}^{"}(x,t) = F(x,t) - EI\left(\frac{F^{"}(x,t)}{\mu AG}\right)$$

Let the static deflection be a weighted superposition of admissible functions (satisfying the boundary conditions), i.e. $z_{st}(x,t) = \sum_{j=1}^{modes} A_j \phi_j(x)$. Premultiplying Eq.6 by $\phi_k(x)$ and integrating over the length, the weights A_j are determined, and the final static deflection is calculated at each time step.

4. Results.

4.1 Free Vibration

Starting with a classical-ended uniform Euler-Bernoulli beam without any axial load, the first complication included is the variation of the end fixity. A simply supported beam has 0% fixity, while a clamped-clamped beam has 100% fixity. The %fixity stands for the ratio of end tensile stresses developed in a beam, as compared to the end tensile stress developed for a clamped-clamped beam. Increasing the fixity increases the modeshape curvature (Fig.4) and the natural frequencies (Table 1) of the beam.

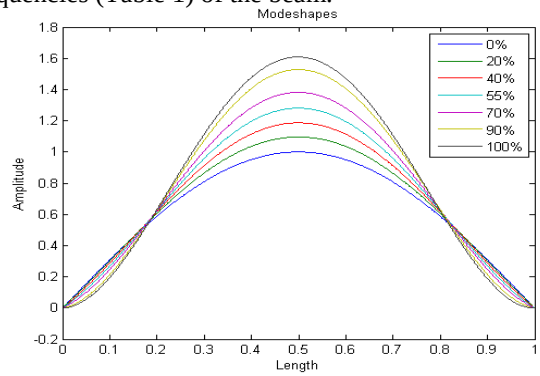

Fig.3 Beam modeshapes for various end fixities.

Table 2 : First 10 natural frequencies of Euler-Bernoulli beams with intermediate fixities.

Fixity / Modes	0%	22%	40%	55%	70%	90%	100%
1	3.1416	3.5768	3.8974	4.1557	4.3737	4.6141	4.7300
2	6.2832	6.5466	6.8077	7.0682	7.3293	7.6682	7.8377
3	9.4248	9.6127	9.8250	10.0657	10.3387	10.7463	10.9739
4	12.5664	12.7120	12.8850	13.1053	13.3749	13.8283	14.1093
5	15.7080	15.8267	15.9769	16.1718	16.4314	16.9148	17.2499
6	18.8496	18.9497	19.0802	19.2561	19.5031	20.0053	20.3804
7	21.9912	22.0778	22.1929	22.3528	22.5867	23.0994	23.5160
8	25.1327	25.2090	25.3120	25.4582	25.6793	26.1969	26.6516
9	28.2743	28.3425	28.4356	28.5700	28.7791	29.2974	29.7872
10	31.1459	31.4775	31.5625	31.6869	31.8847	32.4013	32.9253

Inclusion of axial loads changes the natural frequencies, without affecting the beam modeshapes. Tensile force increases the natural frequencies, while a compressive force reduces them, as shown in Table 3. Inclusion of shear deformation and rotary inertia reduced the natural frequencies, as shown in Table 4.

Table 3 : First 5 natural frequencies of axially-loaded **Euler-Bernoulli beams** with intermediate fixities.

N = -0.8*Pcr	**Fixity**	**0%**	**22%**	**55%**	**70%**	**100%**
Mode	**1**	2.103	3.0391	3.8315	4.0882	4.4706
	2	5.9426	6.2487	6.8298	7.1106	7.6423
	3	9.2082	9.409	9.8875	10.1721	10.8238
	4	12.4064	12.5576	12.964	13.2409	13.9878
	5	15.5809	15.7025	16.0552	16.3196	17.1428
N = Pcr	**Fixity**	**0%**	**22%**	**55%**	**70%**	**100%**
Mode	**1**	3.7355	4.0215	4.475	4.6641	4.9834
	2	6.6433	6.8695	7.3356	7.5771	8.0622
	3	9.6761	9.8504	10.2759	10.5362	11.1531
	4	12.7581	12.8974	13.2757	13.5369	14.257
	5	15.8626	15.9779	16.3141	16.5679	17.3699

Table 4 : First 5 natural frequencies of axially loaded **Timoshenko beams** with intermediate fixities.

N = 0	**Fixity 0%**	**Fixity 55%**	**Fixity 100%**
Mode 1	3.1392	4.1523	4.7162
Mode 2	6.2643	7.0465	7.8104
Mode 3	9.3619	9.9979	10.893
Mode 4	12.4196	12.9518	13.9321
Mode 5	15.4272	15.8825	16.9187
N = -0.8Pcr	**Fixity 0%**	**Fixity 55%**	**Fixity 100%**
Mode 1	2.0966	3.8259	4.4638
Mode 2	5.9214	6.8051	7.6117
Mode 3	9.1421	9.8161	10.7388
Mode 4	12.2556	12.806	13.8055
Mode 5	15.2951	15.7606	16.8107
N = Pcr	**Fixity 0%**	**Fixity 55%**	**Fixity 100%**
Mode 1	3.7338	4.4733	4.981
Mode 2	6.6264	7.3166	8.0384
Mode 3	9.6164	10.2121	11.077
Mode 4	12.6159	13.1273	14.0857
Mode 5	15.5876	16.031	17.0508

Proc. of the Intl. Conf. on Advances in Structural,Civil and Environmental Engineering -- SCEE 2013

ISBN: 978-981-07-6261-2

4.2 Forced Vibration

The first two modes are used to generate the total deflection of the beam, subject to two different configurations of the transient loads. The mode-summation method yields the following matrices for the generalized mass GM, generalized moment of inertia GR, generalized flexural stiffness GK, generalized shear stiffness GS, and generalized axial loads GN (Table 5 and table 6).

Table 5 : GM, GR, GN for 2x2 modes.

GM			**GR**			**GN**	10^7	
	1	**2**		**1**	**2**		**1**	**2**
1	1.8732	-0.0000	**1**	0.0040	-0.0000	**1**	-0.2353	0.1090
2	-0.0000	2.0848	**2**	-0.0000	0.0075	**2**	0.1090	-0.2353

Table 6 : GK, GS for 2x2 modes.

GK			**GS**		
	1	**2**		**1**	**2**
1	$-0.2292*10^7$	$0.0000*10^7$	**1**	$0.4500*10^6$	$-0.0001*10^6$
2	$0.0000*10^7$	$-1.1985*10^7$	**2**	$0.0000*10^6$	$4.9065*10^6$

The principal coordinates $q_j(t)$ have been generated by the numerically stable Euler's implicit-explicit scheme, as functions of time, for different speeds of the transient force. The principal coordinates when premultiplied by the respective modeshapes, and superposed, generates the total beam deflection as a function of space and time z(x,t).

The maximum dynamic deflection is normalized by the maximum static deflection to generate the Dynamic Load Factor (DLF), which is generated as a function of the non-dimensional wetting time τ. The numerator and the denominator may occur at different locations, and at different time instants. The DLF is defines as :

$$DLF = Max\left[\frac{z(x,t)}{Max\left[z_{st}(x,t)\right]}\right].$$

4.2.1 Uniform Load

Fig.5 shows the generalized force for the first five modes of a CC beam, at τ = 0.5, as a function of time. The force is a uniform stretching load, and hence spatially aligns itself only with the odd modeshapes. The even modes give zero generalized force after the load has completely swept across.

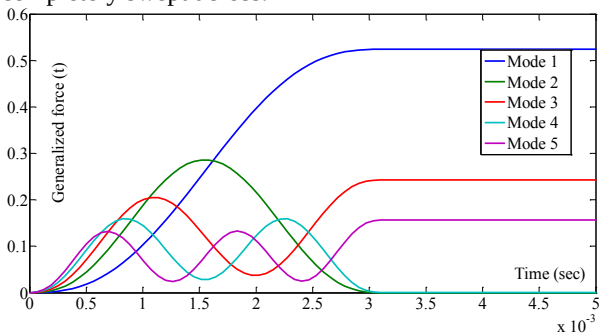

Fig.5 GF vs. time for the first 5 modes of a CC beam, at τ = 0.5.

The dynamic and static deflections at the midpoint of the beam, for the uniform stretching load, as a function of time, for τ = 0.5 and 2.5 are plotted as follows in Fig.6. For τ = 0.5, as the load sweeps across quickly, the maximum static deflection is reached quickly, and the dynamic overshoot is about 90% higher than the corresponding static deflection. For τ = 2.5, as the load sweeps across the beam slowly, the maximum static deflection is reached later, and the dynamic overshoot is hardly 5% of the static mean.

Fig.7 shows the dynamic loading factor DLF vs. τ (the non-dimensionalized wetting time) for a uniform Timoshenko beam, without axial load, for various end fixities and damping ratios ζ. Increase of end fixities makes the beam stiffer (i.e. increases the natural frequencies), and hence stretches the τ-axis if the plot. Larger values of τ indicate a stiffer beam (or massless beam) or a large wetting time, i.e., a slow transition of the moving loads. In this zone of the non-dimensionlized time-scale, the response is quasi-static, i.e. the DLF is around 1.0. Decreasing the τ increases the dynamic behavior of the beam, leading to larger DLF. Here, we have very fast moving loads, or a very tender beam (or massy beam). For τ ≤ 2, the dynamic response becomes increasingly prominent, showing considerable overshoots above the static analysis.

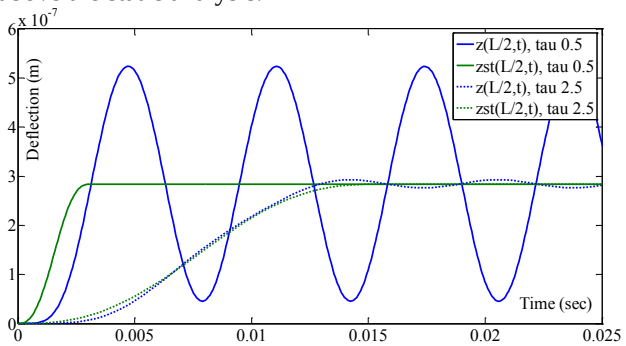

Fig.6 Dynamic z(L/2,t) & static deflection z_{st}(L/2,t) for CC beam, for uniform loading at τ = 0.5, 2.5; for 0% damping.

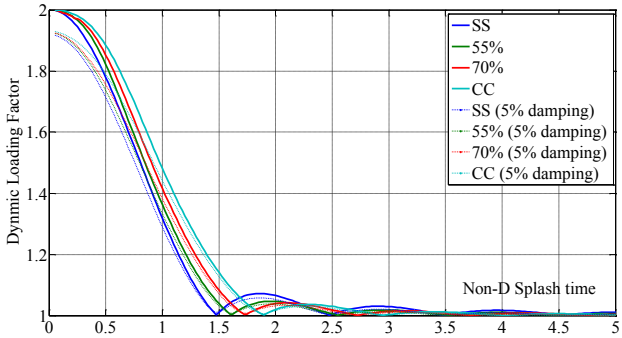

Fig.7 DLF vs. τ for a Timoshenko beam under uniform load, 0% and 5% damping.

Proc. of the Intl. Conf. on Advances in Structural,Civil and Environmental Engineering -- SCEE 2013

ISBN: 978-981-07-6261-2

At smaller τ the DLF steeply rises to asymptote to ~ 2.00, which is the DLF for a uniformly distributed load instantaneously acting on the beam. The response for τ < 1 can be said to be a slamming-response, which is somewhat restricted by the damping. The response at zero damping provides the upper limit of the response characteristic for a range of τ. Inclusion of structural damping reduces the first dynamic overshoot over the static deflection, and hence the dynamic zone of the DLF (0<τ<2) sees a stunted DLF. Damping also smoothens the DLF characteristic in the quasi-static zone.

The DLF become exactly 1.0 at regular intervals : e.g. for a SS beam, DLF = 1.0 at τ = 1.5, 2.5, 3.5, 4.5, and so on. For a CC beam, the first DLF=1.0 occurs at τ = 1.85.

Inclusion of axial tension in the beam vibration analysis is practically relevant, since marine structural members are constantly under axial loads due to static pre-deflections, hogging/sagging of the keel plate, compressive loads on the bulkheads due to derricks, etc. Several members of a marine craft may be pre-stressed due to rolling (during fabrication). The magnitude of the tensile force is equal to the critical buckling load, as given in table. The value of the critical load, as shown in table 7, is known for the classical end conditions, i.e. for SS and CC beams. The critical load magnitude for the intermediate end fixities are calculated through linear interpolation. Greater the end fixity, larger is the critical buckling load.

Table 7 Axial tension applied on the beam

% Fixity	0%	55%	70%	100%
Tension (N)	$\frac{\pi^2 EI}{L^2}$	$\frac{2.65\pi^2 EI}{L^2}$	$\frac{3.1\pi^2 EI}{L^2}$	$\frac{4\pi^2 EI}{L^2}$

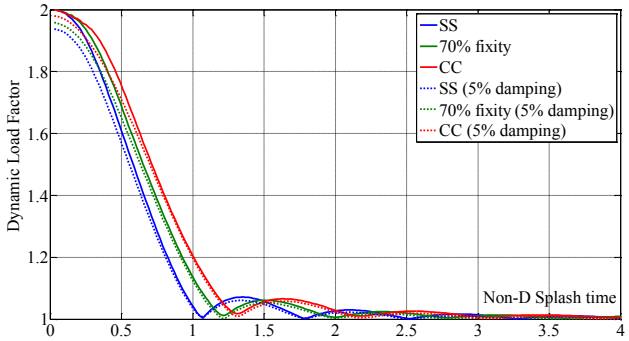

Fig.8 DLF vs. τ for an (tensile) axially loaded Timoshenko beam under uniform load, 0% and 5% damping.

Fig.8 shows the dynamic loading factor DLF vs. τ (the non-dimensionalized wetting time) for a uniform Timoshenko beam, with axial tensile load N, for various end fixities and two damping ratios ζ = 0% and 5%. Axial tension stiffens the dynamic behavior of the beam, thereby squeezing the range of the dynamic behavior of the beam. E.g., for an SS beam, the first DLF = 1 occurs at τ = 1.5 without tension; but it occurs sooner, at τ~1.05, with axial tension. Again, for a CC beam, the first DLF = 1 occurs at τ = 1.85 without tension; but it occurs sooner, at τ~1.3, with axial tension.

By intuition, compression should stretch the τ-scale of the DLF plot, thereby increasing the range of τ which shows dynamic behavior.

Impact Load.

Fig.9(a) shows the sweeping impact load at a deadrise angle β = 5 degree. The keel pressure remains a constant at x = 0 location, while the peak pressure moves across the length of the beam at a speed Vπ/2sinβ. The spatial configuration of the load becomes nearly a uniformly distributed load after a long time. The generalized force for the impact stretching load, against the five modeshapes, as a function of time, at τ = 0.5, is plotted as follows in Fig.9(b). The force aligns itself spatially with the odd modes, while the even modes produce a zero generalized force after the impact has swept across. Fig.10 shows the corresponding dynamic and static deflections at the midpoint of the beam, as functions of time, for a simply-supported (SS) Timoshenko beam, at a deadrise angle of 5 degrees, 0% damping.

Fig.11 shows the dynamic deflection and the negative of the static deflection, at five different time instants as a function of length at τ = 0.5, for a deadrise angle of β = 5 degrees. For 0 < τ < 0.5, the impact already sweeps through and the static deflection already peaks, before the dynamic deflection rises to its maximum.

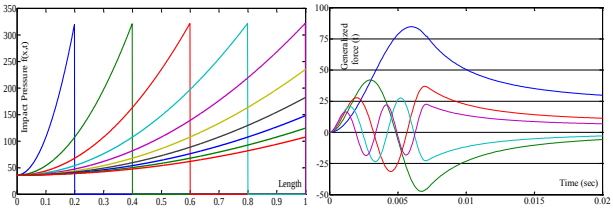

Fig.9 Transient impact force F(x,t) and generalized force GF(t) at β = 5, τ = 0.5, for a SS beam.

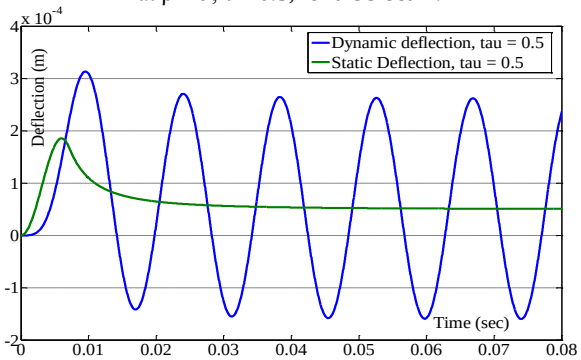

Fig.10 Dynamic z(L/2,t) & static deflection z_{st}(L/2,t) for SS beam, for impact loading at τ = 0.5; for 0% damping, at β = 5 degrees.

Proc. of the Intl. Conf. on Advances in Structural,Civil and Environmental Engineering -- SCEE 2013

ISBN: 978-981-07-6261-2

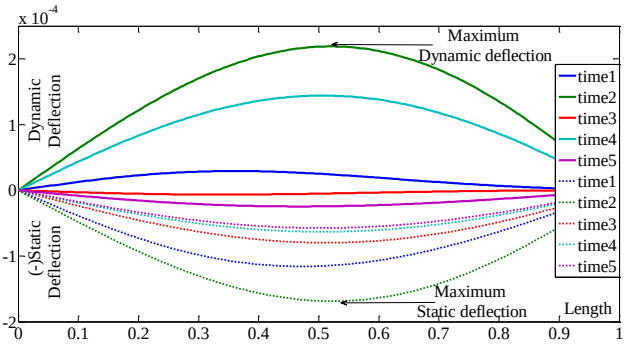

Fig.11 Dynamic deflection and (-) Static deflection at β = 5, τ = 0.5, for a SS beam.

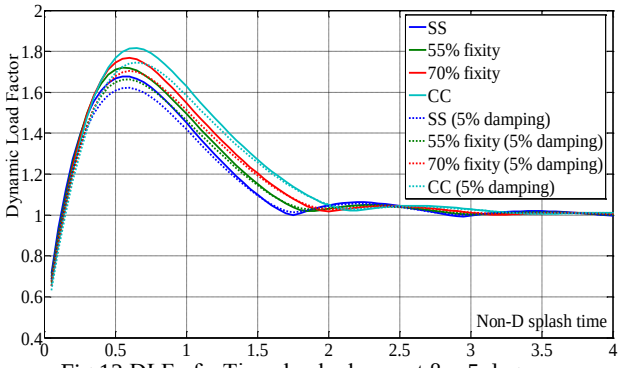

Fig.12 DLF of a Timoshenko beam at β = 5 degrees.

Fig.12 shows the DLF of a Timoshenko beam, at a deadrise angle β = 5 degrees; at a two different damping ratios ζ = 0%, 5%. The time-scale is non-dimensionalized with respect to the deadrise angle, and hence the DLF characteristic is almost the same for a range of deadrise angles. Between $1 < \tau < 2.5$, a smaller deadrise angle produces a greater DLF due to more severe and concentrated impact pressure. A greater deadrise angle smears and spreads the impact pressure distribution, thereby producing a slightly smaller DLF. Beyond $\tau = 2.5$, all the deadrise angles produce a quasi-static behavior.

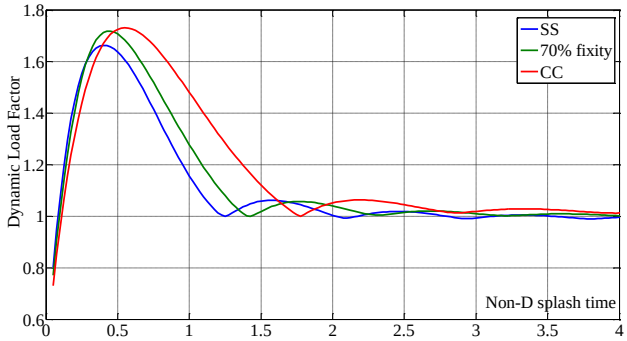

Fig.13 DLF vs. τ for an (tensile) axially loaded Timoshenko beam under impact load, 0% damping, β = 5 degrees.

At very low values of τ, the DLF sharply drops and asymptotes to zero. The load sweeps across too fast for the beam to dynamically react, whereas the static analysis over-predicts the deflection. Hence their ratio decimates, for all end fixities and axial loads. Damping reduces the maximum DLF.

Fig.13 shows the dynamic loading factor DLF vs. τ (the non-dimensionalized wetting time), at β = 5 degrees, for a uniform Timoshenko beam, with axial tensile load N (given in Table 7), for various end fixities and no damping. Tension compresses the τ-axis, with the dynamic response zone shortening to $0.5<\tau<1.5$. In this zone, greater end fixity produces a larger dynamic amplification. For $\tau<0.5$, the behavior is consistent for all end fixities and axial loads.

5. Conclusions.

The designer aims to design structure with the boundary conditions and, stiffness and damping such that the composite time-scale τ is greater than 2.5 for the most probable impact velocities. To operate in the quasi-static range, the forcing speed should be low, or the natural frequency of the beam must be high. A craft meant for inland operations (i.e. calm waters) can afford a softer structure, where slamming is less common. A sea-going vessel, on the other hand would require a stiffer bottom structure to ensure a quasi-static response. High-speed vessels, though use mostly in calm waters, needs stiffer material, since the varying dynamic lifts (partially supporting the craft weight) cause repeated slamming of the bow at high impact speeds.

Nomenclature

x	Independent space variable along the beam
T	Independent variable in time
z(x,t)	Dynamic flexural deflection of the beam
$z_{st}(x,t)$	Dynamic flexural deflection of the beam
Φ(x,t)	Pure-bending slope of the beam
z_{st}	Static flexural deflection of the beam
L	Length of the beam
ρ	Density of the beam material
E	Elastic modulus of the beam material
I	Second moment of area of the beam cross-section about the horizontal neutral axis.
G	Shear modulus of the beam material
μ	Shear correction factor (5/6 for rectangular cross-section)
A	Cross-sectional area of the beam
$K_{\theta L}$	Spring constant on the left end
$K_{\theta R}$	Spring constant on the right end
$\phi_j(x)$	Beam modeshape
$\psi_j(x)$	Pure bending slope modeshape
δ_j,γ_j	j^{th} frequency parameter pair for Timoshenko beam.
$q_j(t)$	Principal coordinate
F(x,t)	External transient load

ISBN: 978-981-07-6261-2

ω_{n1}	Fundamental natural frequency of the beam
T_{n1}	Fundamental natural period of the beam
Tsp	Splash time
τ	Non-D splash time
V	Vertical impact velocity of slamming
β	Deadrise angle of the craft
DLF	Dynamic Loading Factor

References

[1] Bokaian, A., "*Natural frequencies of beams under tensile axial loads*", Journal of Sound and Vibration (1990), 142(3), 481-498.

[2] Lin, Y.H., "*Vibration analysis of Timoshenko beams traversed by moving loads*", Journal of Marine Science and Technology, Vol.2, No.1, pp.25-35 (1994).

[3] T.P.Chang, "*Deterministic and random vibration of an axially loaded Timoshenko beam resting on an elastic foundation*", Journal of Sound and Vibration (1994), 178(1), 55-66.

[4] S.H.Farchaly and M.G.Sgebl, "*Exact frequency and modeshape formulae for studying vibration and stability of Timoshenko beam system*", Journal of sound and vibration (1995) 180(2), 205-227.

[5] R.T.Wang, "*Vibration of multi-span Timoshenko beams to a moving force*", Journal of Sound and Vibration (1997) 207(5), 731-742.

[6] Majkut, L., "*Free and forced vibrations of Timoshenko beams described by single difference equation*", Journal of theoretical and applied mechanics, 47, 1, pp.193-210, Warsaw 2009.

[7] Datta N., Kim D. and Troesch A.W., "*Hydrodynamic impact-induced vibration characteristics of a uniform Euler-Bernoulli beam*", International symposium on vibro-impact dynamics of ocean systems and related problems, Troy, Michigan, Oct 2008.